Acetylcholine Induces Fibrogenic Effects via M2/M3 ACh Receptors in NASH and in Primary Human Hepatic Stellate Cells

Maelle L. Morgan[1], Barbara Sigala[1], Junpei Soeda[1], Paul Cordero[1], Vi Nguyen[1], Chad McKee[1], Angelina Mouraliderane[1], Manlio Vinciguerra[1,2,3*], Jude A. Oben[1,4]

[1] University College London, Institute for Liver and Digestive Health, Royal Free Hospital, Rowland Hill Street, NW3 2PF, London, UK; [2] Gastroenterology Unit, Department of Medical Sciences, Casa Sollievo della Sofferenza Hospital, San Giovanni Rotondo, Viale dei Cappuccini, 71013, Italy; [3] Interdisciplinary Biomedical Research Centre, School of Science and Technology, Nottingham Trent University, NG11 8NS, Nottingham, United Kingdom; [4] Guy's and St Thomas' National Health Service Foundation Trust, SE1 7EH, London, United Kingdom.

Corresponding author:

Manlio Vinciguerra, B.Sc., M.Sc., Ph.D., University College London, Institute of Liver and Digestive Health, Royal Hospital, Free London, NW3 2PF, UK. E-mail: m.vinciguerra@ucl.ac.uk ; phone: +44 020-7433-2874.

Short title: Acetylcholine and hepatic stellate cells

This article has been accepted for publication and undergone full peer review but has not been through the copyediting, typesetting, pagination and proofreading process which may lead to differences between this version and the Version of Record. Please cite this article as doi: 10.1111/jgh.13085

Abstract

Background: the parasympathetic nervous system (PNS), via neurotransmitter Acetylcholine (ACh), modulates fibrogenesis in animal models. However, the role of ACh in human hepatic fibrogenesis is unclear. *Aims:* we aimed to determine the fibrogenic responses of human hepatic stellate cells (hHSC) to ACh and the relevance of the PNS in hepatic fibrosis in patients with non-alcoholic steatohepatitis (NASH). *Methods:* primary hHSC were analysed for synthesis of endogenous ACh and acetylcholinesterase (AChE), and gene expression of choline acetyltransferase (ChAT) and muscarinic acetylcholine receptors (mAChR). Cell proliferation and fibrogenic markers were analysed in hHSC exposed to ACh, Atropine (Atrop), Mecamylamine (Mec), methoctramine and 4-Diphenylacetoxy-N-methylpiperidine methiodide (4-DAMP). MAChR expression was analysed in human NASH scored for fibrosis. *Results:* we observed that hHSC synthesise ACh and AChE, and express ChAT and M1-M5 mAChR. We also show that M2 was increased during NASH progression, while both M2 and M3 were found upregulated in activated hHSC. Furthermore, endogenous ACh is required for hHSC basal growth. Exogenous ACh resulted in hHSC hyperproliferation via mAChR and PI-3K and MEK signalling pathways, as well as increased fibrogenic markers. *Conclusion:* We show that ACh regulates hHSC activation via M2 and M3 mAChR involving the PI-3K and MEK pathways in vitro. Finally, we provide evidence that the PNS may be involved in human NASH fibrosis.

Keywords:

Liver disease

Fibrosis

Parasympathetic nervous system

Introduction

It is well established that hepatic stellate cells (HSC) are the principal fibrogenic cell type of the liver. Following injury, inflammatory cytokines convert the quiescent HSCs into activated HSC, which are highly proliferative and exhibit increased collagen type-1 and α-smooth muscle actin (ASMA) deposition, culminating in ECM accumulation and fibrosis[1]. Hepatic fibrosis is the end stage of many chronic liver diseases, with non-alcoholic fatty liver disease (NAFLD) the most common form of chronic liver disease in the Western world[2, 3]. NAFLD is an infiltration of fat into the parenchyma of the liver, which is tightly related to obesity, insulin resistance, metabolic syndrome and aging[4-7]. Ongoing inflammation and impaired wound healing responses progress NAFLD to the more severe disease non-alcoholic steatohepatitis (NASH)[8, 9], which may in turn progress to advanced fibrosis, cirrhosis and end-stage liver disease[10, 11]. The mechanisms underlying this progression to cirrhosis are currently unclear. Recent evidence suggests the parasympathetic nervous system (PNS) plays a role in the regulation of cell proliferation and wound healing involved in fibrogenic pathologies of the skin and airway epithelial cells[12, 13]. The cholinergic pathway also has implications in modulating inflammation in multiple disease states including atopic dermatitis, and cystic fibrosis[14, 15]. Further evidence also suggests dietary fat modulates inflammatory processes via the cholinergic pathway[16-19], showing the PNS may be implicated in obesity and associated metabolic disorders such as NAFLD.

The PNS has also been implicated in murine hepatic fibrogenesis. In the carbon tetrachloride (CCl_4) murine model of liver injury, AChE positive nerve fibres are shown to occur in the fibrous septa of cirrhotic rat livers and these fibres form nerve terminal/myofibroblast complexes[20]. Furthermore, results from our group show that murine hepatic stellate cells (mHSC) are highly proliferative and have increased COL1A2 expression in response to exogenous acetylcholine, as well as nicotine[21, 22]. Concurrently, it was recently demonstrated

that culture activated mHSC express mAChR[22]. Other *in vivo* studies showed that cholinergic denervation reduces mHSC activation and proliferation in CCl_4 induced liver fibrosis in rats[23]. Similar findings have also been suggested in humans, though results are conflicting[24]. These studies suggest a potential role for the PNS in regulating human hepatic fibrogenesis, particularly in the setting of NASH fibrosis, and further investigations are warranted. The aim of this study was to determine whether hHSC express mAChR, respond in a fibrogenic manner to acetylcholine and to determine the relevance of the PNS in hepatic fibrosis in patients diagnosed with NASH.

Methods

Human Hepatic Stellate Cell Isolation and Treatment

Human liver tissue was acquired with approval by the appropriate local Ethical Committee and patient consent. Cell separation was conducted via collagenase and DNase perfusion[25]. Non-parenchymal cells including HSC were subsequently isolated[26]. Cells were plated at a density of $5x10^4$ cm^2 in RPMI medium containing penicillin 100 u/mL and streptomycin 100 µg/mL (Gibco, Invitrogen, UK), 10% Foetal Bovine Serum (FBS) (Gibco, Invitrogen, UK) and 2-ME (Gibco, Invitrogen, UK), and cultured to activation to day 15 on uncoated plastic flasks. Cell identity was confirmed by autofluorescence, and the expression of two well-accepted HSC markers, alpha smooth muscle actin (AMSA) and glial fibrillary acidic protein (GFAP) by immunocytochemistry. When required, activated cells were exposed to drug treatment (Table 1).

Acetylcholine and Acetylcholinesterase Activity Assay

Activated hHSC were plated at a density of 5000 cells per well in a 96 well plate in RPMI as described above without 2-ME. Cell supernatant was collected after 48hours and

acetylcholine was measured using Amplex Red Acetylcholine/Acetylcholinesterase Assay Kit (Invitrogen, UK). Cells were trypsinized and counted using a NucleoCounter. Cells were also plated out as above, sonicated and centrifuged at 13,000 rpm for 20 minutes at 4°C and the supernatant collected. Acetylcholinesterase was measured in the sonicated cell supernatant using the same assay kit, since AChE is contained within the cell cytoplasm[27]. Fluorescence was measured in a fluorescence microplate reader (Anthos HT III) at excitation 530-560 nm and emission 590 nm, and readings read off standard curve minus controls. Acetylcholine and acetylcholinesterase levels were measured as a ratio of cell numbers.

Cell Proliferation Assay

Activated hHSC were plated at a density of 5000 cells per well in a 96 well plate in RPMI containing 10% FBS. Cholinergic agonists and antagonists from Table 1 were added to the medium for 48hours. Cell proliferation assay was conducted as per protocol using WST-8 cell counting kit (Dojindo Molecular Technologies, NBS Biologicals, UK). Optical densities were read with an Emax precision microplate reader (Anthos HT III) at 450nm.

Apoptosis assay

Activated hHSC were plated at a density of $1x10^6$ cells per T25 flask. Activated cells were exposed to cholinergic agonists and antagonists from Table 1 in RPMI containing 10% FBS for 48hours. Cells were lightly trypsinized and an apoptotic activity was performed with the Vybrant (annexin V) apoptosis assay kit 2 (Molecular Probes, Invitrogen) as per the manufacturer's instructions. FACS analysis was performed using FACS Calibur.

RNA Isolation and RT-PCR

Isolation of total RNA from cells and homogenised liver tissue was performed using TRIzol™ Reagent (Invitrogen, UK) as per manufacturer's instructions as previously performed[28]. Primers were designed using Primer3 (see Table 2). RNA from samples was reversed transcribed and amplified via PCR using Superscript III One-Step RT-PCR System (Invitrogen, UK) and SYBR Green^{ER} (Invitrogen, UK). Reactions were performed on Rotorgene thermal cycler (Rotorgene RG 3000, Corbett Research, Australia). cDNA was amplified (denaturation at 94°C for 15 sec, annealing temperatures as shown in Table 2 for 30 sec, extension at 72°C for 60 sec). A melt curve analysis (50–90°C with a heating rate of 1° per second) confirmed the amplification of specific PCR products and the absence of non-specific amplification or primer-dimers. The amount of transcript was calculated and expressed as the difference relative to the control gene GAPDH ($2^{-\Delta\Delta Ct}$, where Ct represents the difference in threshold cycles between the target and control genes).

Immunocytochemistry

Immunocytochemistry was performed on activated hHSC. Cells were plated on sterilized cover slips at a density of $5x10^3$ cells per well of a 24well plate (Nunc, Thermo Fisher Scientific, UK) in RPMI media and grown to 50% confluence. Cells were washed with chilled PBS and fixed with methanol-acetone (50/50 v/v). The fixed cells were washed in a blocking solution containing 10% goat serum (Gibco, Invitrogen, UK) and 0.3% BSA (10% in DPBS) in PBS for 1hr at room temperature. Primary antibody diluted in block buffer was added for 1hr at room temperature. Final antibody dilution was anti-ASMA 1:400 (Santa Cruz, CA, US) and ChAT 1:100. Secondary antibodies conjugated to FITC and Texas Red were diluted in block buffer at 1:5000 and applied to cells for 1hr at room temperature. Slides

were mounted in VectraShield with DAPI (Vector Laboratories) on cover slips and examined with a Zeiss LSM 510 Meta Confocal Microscope[29].

MAChR expression in NASH fibrosis

Whole liver NASH samples were supplied from the Laboratory of Morphology and Molecular pathology of the University of Leuven (Belgium) following the local Ethics Committee approval in accordance with the Helsinki Declaration. Written and informed consent was obtained for all participants. Right lobule liver biopsies were conducted and histologically scored for NASH on the Brunt fat content scaling system (n=3), confirming NASH, as well as scored for fibrosis on the METAVIR fibrosis score system[30]. The biopsies were snap frozen in liquid nitrogen and stored at -80°C. MAChR expression was analysed in these samples via RT-PCR.

Statistical Analysis

All experiments were performed in duplicate from 3 separate experiments and analysed using statistical program GraphPad Prism 6 (GraphPad Prism, San Diego, USA). Statistical significance was calculated using the Mann-Whitney t-test and a p value of <0.05 was considered significant (*) a p value of <0.01 considered highly significant (**) and a p value of <0.001 considered very highly significant (***). Results are represented as means ± SEM.

Results

Human HSC express ChAT, and synthesise ACh and AChE, require ACh as an endogenous growth factor

Until now, there was no data demonstrating the potential for hHSC to express and synthesise the cholinergic enzymes, ChAT, ACh and AChE. Here, we were able to demonstrate via confocal microscopy, that activated HSC cells expressed ChAT protein, found to be located in bundles and spread diffusely within the cell cytoplasm (Texas Red fluorescence), where ASMA (FITC), which is expressed abundantly, is used as a control protein to confirm the cell type and activated phenotype (Fig. 1A). We further demonstrated that activated hHSC cultured for 48 hours, release ACh at 25uM per $1x10^6$ cells or 0.25pM per cell into cell culture supernatant. hHSC with cytoplasmic AChE, were sonicated and the supernatant analysed for AChE. Enzyme assay found hHSC to release cytoplasmic AChE at a concentration of 180mU/mL per $1x10^6$ cells (Fig. 1B). Since hHSC synthesize acetylcholine and express acetylcholine receptors, we next determined whether the cells respond functionally to endogenous ACh. Cells cultured for 48hours with mAChR antagonist atropine (Atr 10uM), show basal cell growth inhibition (20% +/- 7%) as determined by proliferation assay, almost to the same extend as the cells cultured in serum free conditions (Fig. 1C).

Activated hHSC express acetylcholine receptor mRNAs and protein

Real time qPCR was performed to characterize cholinergic gene expression in activated hepatic stellate cells as well as whole liver and hepatocytes. It was found that activated human stellate cells express genes for all mAChR including mRNA for M2 > M3 > M1 > M4 > M5 (Fig. 2A). HHSC expressed predominantly M2 and M3 muscarinic ACh receptors (Fig. 2A). To confirm that M receptors expression in hHSC was not variable between human donors, expression of the ACh receptors was confirmed in 3 sets of isolated cells, and

although slight variability in receptor expression occurred between cells, these were not significant (*data not shown*). Human hepatocytes expressed mRNA for all mAChR with M3=M2 > M1=M4=M5, while whole liver scored with F4 fibrosis expressed all mRNA mAChR with M2 > M3 > M1 > M5 > M4 (Fig 2A). To confirm the expression at a protein level, M3 protein expression was analysed via immunofluorescence and confocal microscopy. Confocal microscopy of activated HSC showed the cells express M3 mAChR protein (Texas Red fluorescence) located in bundles, which may be consistent with a localisation in the Golgi apparatus in the perinuclear region of the cell cytoplasm, with ASMA (FITC) as a control for activated HSC phenotype (Fig. 2B).

Acetylcholine stimulates hHSC proliferation via cell surface M2 and M3 (Gαq/11 protein) mAChR

To assess the functionality of the cholinergic receptors, cells were cultured with various concentrations of ACh +/- atropine and cell proliferation was measured. Exogenous acetylcholine applied to cells was found to induce hHSC proliferation in a dose dependent manner with peak proliferation at 10nM-1uM (Fig. 3A). At 1uM, proliferation was increased to 140% +/- 2% of the FBS control. ACh at a dose of 1uM, which induced hHSC proliferation, was blocked by 10uM Atr to 90.7% +/-8% of FBS control (Fig. 3B), although this did not inhibit growth below the negative control (serum free). Since hHSC responded to acetylcholine with increased proliferation, an apoptosis assay was conducted to determine the effects of exogenous ACh on hHSC apoptosis. Human HSC exposed to ACh 1uM showed decreased stellate cell apoptosis by 21% +/- 2.8%. This effect was blocked when ACh 1uM and Atr 10uM were applied simultaneously (Fig. 3C). This further confirms that ACh not only directly increased cell survival, but also inhibited the normal programmed cell death of the stellate cells resulting in increased survival of the cells. The high expression of M2 and

M3 mAChR in activated hHSC as well as the increase in receptor expression in fibrotic liver suggests that these receptors may be directly involved with fibrogenesis. Due to hHSC endogenous Ach activity, atropine could inhibit Ach and increase the apoptotic stage. Surprisingly, we found a lack of effect of supplied Atr on endogenous Ach (Figure 3C), possibly related to cellular membrane permeability to Atropine or intracellular active Ach concentration. As acetylcholine supplementation triggered hHSC proliferation (Figure 3A and 3B), we focused our attention in this extra Ach role, rather than in the internal basal concentration. Therefore, we conducted further experiments to determine if blocking these specific receptors could inhibit ACh induced proliferation and collagen gene expression. Cells were exposed to ACh 1 uM as well as the M2 mAChR antagonist methoctramine, which antagonises the receptors at pM to nM concentrations, as well as M3 mAChR antagonist 4-DAMP. Here, we show that both methoctramine and 4-DAMP inhibit ACh induced proliferation from 140 +/- 2% to 95 +/- 20% and 98 +/-18% (Fig. 3D) respectively of the % response to FBS control.

Acetylcholine stimulates hHSC proliferation via intracellular activation of the PI-3 kinase and MEK cell survival pathways

To further characterise the intracellular mechanism by which hHSC proliferation occurs, cells were exposed to cell survival pathway inhibitors in the presence of ACh. Hepatic stellate cells were exposed to ACh 1uM, as well as antagonists for Gαi/o-protein (PT), PI3-kinase (WT), MEK (PD), p38MAP-kinase (SB), and PKC (RO). We found that blocking both the PI3-K and MEK cell survival pathways, resulted in inhibited ACh induced proliferation by 35 +/- 5% and 42 +/- 4% respectively, suggesting ACh induced proliferation primarily occurs via PI3-K and MEK, though PKC antagonist also had a slight response inhibiting proliferation 20 +/- 8% (Fig. 4). The results obtained suggested the involvement of the Gαi/o-

protein couple receptor antagonist pertussis toxin. In this respect, M2 and M4 are Gio proteins, while M1, M3 and M5 are Gαq/11-protein receptors. Thus, the lack of effect of PT on Ach-induced hHSC proliferation (Fig. 4) could suggest no M2 or M4 involvement in this process. However, this result should be considered with some caution, as our findings highlight the importance of M2 in hHSC proliferation and as there are other multiple potential Gio targets for PT (ie. adrenergic, cannabinoid, glutamate or serotonin receptors among others).

Acetylcholine Induces hHSC TGF-B and Collagen Fibrogenesis via M2 and M3 mAChR

hHSC induced fibrogenesis involves both cell proliferation and overproduction of matrix proteins including collagens. Here, we analysed the effects of ACh exposure on the production of matrix proteins. The conical pathway of collagen production occurs via TGF-B. To determine whether ACh alters collagen production, cells were exposed to ACh and analysed for changes in TGF-B and COL1A2 expression. TGF-B gene expression was significantly upregulated in ACh 1μM treated cells to 200% +/- 23.4% of the FBS control (Fig. 5A), as was COL1A2 to 208% +/- 8.8% (Fig. 5B). COL1A2 expression was also inhibited by methoctramine and 4-DAMP from 208% +/- 8.8% to 170 +/- 9% and 173 +/- 21% of the FBS control (Fig. 5C).

M2 Ach receptor is upregulated in hHSC activation and in NASH fibrosis

As our data suggested the importance of M2 and M3 mAChR expression and function in hHSC proliferation and fibrogenesis, we analysed their expression levels at the stage of activation of hHSC, from quiescent to activated phenotypes. It is already known that ASMA gene expression increases in cell activation from cells cultured from day 0 to day 15, a

defining characteristic of the cell type. Here, we demonstrated that M2 and M3 mAChR receptor expression increases in isolated hHSC (Fig. 6A). With these results, we next attempted to clarify the expression pattern of mAChR in vivo. Using whole liver biopsy samples from patients diagnosed with NASH and scored for fibrosis using the METAVIR fibrosis scoring system, we further demonstrated that as the fibrosis score rose from F0 to F4, ASMA gene expression which was used to confirm fibrosis of the samples increased significantly, as did M2 receptor gene expression, which significantly increased from 38% +/- 12% in F0 samples to 250% +/- 48% in the F4 samples compared to GAPDH (Fig. 6B). Interestingly, M3 receptor expression remained unchanged between F0, F3 and F4, although expression levels in all samples were high at 303-398% (data not shown).

Discussion

This paper demonstrates via multiple techniques the importance of acetylcholine in regulating human hepatic stellate cell growth and activation. For the first time, we show that cultured hHSC produce ChAT and AChE, as well as secreting ACh, and that basal cell growth was inhibited when cultured with atropine. This demonstrates the ability of hHSC to produce and respond to endogenous acetylcholine, suggesting acetylcholine is an autocrine growth factor for hepatic stellate cells. To characterise these cells further, we showed that isolated hHSC express receptors of the PNS including mAChR M2 > M3 > M1 > M4 > M5. This is similar to the expression pattern seen in a recent publication of a murine model of hepatic fibrosis with HSC expressing M2>M3 mAChR. This expression pattern has also been reported in other human cell types with fibrogenic potential, including human lung fibroblasts and human scleral fibroblasts[31, 32], suggesting that collectively, the role of the PNS in fibroblast regulation is likely to be significant. We also demonstrated that gene expression of M2 and M3 were upregulated with activation of hHSC, suggesting that they play an important role in

hepatic fibrogenesis. In addition, M2 expression increased in parallel with NASH progression in human biopsies.

We further demonstrated that cell exposure to exogenous ACh induced hyper-proliferation of hHSC above that of basal cell growth as well as upregulating fibrotic markers TGF-B and COL1A2 gene expression. It appears that this process occurs via ACh binding M2 and M3 mAChR, since blocking these receptors with methoctramine and 4-DAMP inhibited cell proliferation and reduced fibrotic markers to near control levels. These results are also consistent with others findings showing that murine HSC in vitro responds in a proliferative manner to ACh via M2 mAChR pathways[33]. This would suggest that ACh binding to M2 and M3 receptors in particular may be what stimulates the conversion of quiescent HSC into fibroblast phenotypes. Surprisingly, we detect M3 in bundles, indicating a possible localisation in the Golgi apparatus in the perinuclear region of the cell cytoplasm. In this regard, upon folding in the endoplasmic reticulum, proteins are driven to Golgi for maturation and later mobilization to their final functional locations. Furthermore, Golgi secretion granules could be fused with the external membrane. In neurons, although muscarinic receptors are usually located in cell surface, it has been described a cholinergic-induced subcellular redistribution of muscarinic receptors to endoplasmic reticulum and Golgi complex[34].

We also found that ACh induced proliferation occurs via the intracellular signalling pathways involving PI-3K, MEK and PKC. Interestingly, this pathway of fibrogenesis is similar to that demonstrated in muscarinic induced human lung fibroblast proliferation in airway remodelling[35], as well as other conditions of cellular hyper-proliferation, including a multitude of solid tumours such as HCC[36-38]. This pathway may be a significant therapeutic target in hepatic fibrogenesis and therefore, warrants further investigation.

In human whole liver samples of NASH fibrosis, our results showed that M2 receptor expression was increased with severity of fibrosis. This suggests in vivo, that M2 may be involved in fibroblastic changes in NASH, particularly since HSC are the predominant cells causing hepatic fibrosis, and we have also shown in vitro that hHSC express M2. It is important to point out that the implications of altered PNS signalling in the liver is highly relevant, since dietary fat directly stimulates the cholinergic anti-inflammatory pathway via the vagal nerve[18, 19], suggesting a plausible link between a high fat diet, the cholinergic system and fibrosis in NASH. This theory may also be relevant in the setting of progression to fibrosis post-liver transplantation where PNS innervation is permanently severed.

In summary, cholinergic transmission in the liver is a novel explanation for the development of hepatic fibrogenesis. Our findings suggest pathological implications for ACh induced fibrogenesis via mAChR in primary human HSC and as well as in human NASH, and may be a potential therapeutic target.

Acknowledgements

Liver samples were kindly supplied by Dr Clare Selden, UCL-Institute of Liver and Digestive Health, University College London and Professor Brian Davidson, Department of Surgery, Royal Free Hospital, London in conjunction with the North Hampshire Hospital, Basingstoke and Royal Free Hospital, London. Whole liver NASH samples were kindly supplied by Dr Sara Vander Borght, Laboratory of Morphology and Molecular Pathology, University of Leuven, Belgium. This work was funded by the Wellcome Trust (Jude A. Oben) and by the Associazione Italiana per laRicerca sul Cancro (MFAG-AIRC, n.13419).

References

1. Friedman SL. Hepatic stellate cells: protean, multifunctional, and enigmatic cells of the liver. Physiol Rev 2008; 88: 125-172.

2. Lopez-Velazquez JA, Silva-Vidal KV, Ponciano-Rodriguez G, Chavez-Tapia NC, Arrese M, Uribe M, et al. The prevalence of nonalcoholic fatty liver disease in the Americas. Ann Hepatol 2014; 13: 166-178.

3. Vernon G, Baranova A, Younossi ZM. Systematic review: the epidemiology and natural history of non-alcoholic fatty liver disease and non-alcoholic steatohepatitis in adults. Aliment Pharmacol Ther 2011; 34: 274-285.

4. Armstrong MJ, Adams LA, Canbay A, Syn WK. Extrahepatic complications of nonalcoholic fatty liver disease. Hepatology 2014; 59: 1174-1197.

5. Podrini C, Borghesan M, Greco A, Pazienza V, Mazzoccoli G, Vinciguerra M. Redox homeostasis and epigenetics in non-alcoholic fatty liver disease (NAFLD). Curr Pharm Des 2013; 19: 2737-2746.

6. Sheedfar F, Di Biase S, Koonen D, Vinciguerra M. Liver diseases and aging: friends or foes? Aging Cell 2013; 12: 950-954.

7. Vinciguerra M. Old age and steatohepatitis: a dangerous liaison? Hepatology 2013; 58: 830-831.

8. Ekstedt M, Franzen LE, Mathiesen UL, Thorelius L, Holmqvist M, Bodemar G, et al. Long-term follow-up of patients with NAFLD and elevated liver enzymes. Hepatology 2006; 44: 865-873.

9. Rizzo M, Montalto G, Vinciguerra M. Editorial: Exploring Lipid-related Treatment Options for the Treatment of NASH. Curr Vasc Pharmacol 2014; 12: 741-744.

10. Fassio E, Alvarez E, Dominguez N, Landeira G, Longo C. Natural history of nonalcoholic steatohepatitis: a longitudinal study of repeat liver biopsies. Hepatology 2004; 40: 820-826.

11. Michelotti GA, Machado MV, Diehl AM. NAFLD, NASH and liver cancer. Nat Rev Gastroenterol Hepatol 2013; 10: 656-665.

12. Hana A, Booken D, Henrich C, Gratchev A, Maas-Szabowski N, Goerdt S, et al. Functional significance of non-neuronal acetylcholine in skin epithelia. Life Sci 2007; 80: 2214-2220.

13. Kummer W, Krasteva-Christ G. Non-neuronal cholinergic airway epithelium biology. Curr Opin Pharmacol 2014; 16: 43-49.

14. Wessler I, Bittinger F, Kamin W, Zepp F, Meyer E, Schad A, et al. Dysfunction of the non-neuronal cholinergic system in the airways and blood cells of patients with cystic fibrosis. Life Sci 2007; 80: 2253-2258.

15. Wessler I, Reinheimer T, Kilbinger H, Bittinger F, Kirkpatrick CJ, Saloga J, et al. Increased acetylcholine levels in skin biopsies of patients with atopic dermatitis. Life Sci 2003; 72: 2169-2172.

16. de Haan JJ, Hadfoune M, Lubbers T, Hodin C, Lenaerts K, Ito A, et al. Lipid-rich enteral nutrition regulates mucosal mast cell activation via the vagal anti-inflammatory reflex. Am J Physiol Gastrointest Liver Physiol 2013; 305: G383-391.

17. Gautam D, Ruiz de Azua I, Li JH, Guettier JM, Heard T, Cui Y, et al. Beneficial metabolic effects caused by persistent activation of beta-cell M3 muscarinic acetylcholine receptors in transgenic mice. Endocrinology 2010; 151: 5185-5194.

18. Pavlov VA, Tracey KJ. The vagus nerve and the inflammatory reflex--linking immunity and metabolism. Nat Rev Endocrinol 2012; 8: 743-754.

19. Tracey KJ. Physiology and immunology of the cholinergic antiinflammatory pathway. J Clin Invest 2007; 117: 289-296.

20. Akiyoshi H, Terada T. Mast cell, myofibroblast and nerve terminal complexes in carbon tetrachloride-induced cirrhotic rat livers. J Hepatol 1998; 29: 112-119.

21. Oben JA, Yang S, Lin H, Ono M, Diehl AM. Norepinephrine and neuropeptide Y promote proliferation and collagen gene expression of hepatic myofibroblastic stellate cells. Biochem Biophys Res Commun 2003; 302: 685-690.

22. Soeda J, Morgan M, McKee C, Mouralidarane A, Lin C, Roskams T, et al. Nicotine induces fibrogenic changes in human liver via nicotinic acetylcholine receptors expressed on hepatic stellate cells. Biochem Biophys Res Commun 2012; 417: 17-22.

23. Lam HB, Yeh CH, Cheng KC, Hsu CT, Cheng JT. Effect of cholinergic denervation on hepatic fibrosis induced by carbon tetrachloride in rats. Neurosci Lett 2008; 438: 90-95.

24. McCuskey RS. Anatomy of efferent hepatic nerves. Anat Rec A Discov Mol Cell Evol Biol 2004; 280: 821-826.

25. Selden C, Chalmers SA, Jones C, Standish R, Quaglia A, Rolando N, et al. Epithelial colonies cultured from human explanted liver in subacute hepatic failure exhibit hepatocyte, biliary epithelial, and stem cell phenotypic markers. Stem Cells 2003; 21: 624-631.

26. Sigala B, McKee C, Soeda J, Pazienza V, Morgan M, Lin CI, et al. Sympathetic nervous system catecholamines and neuropeptide Y neurotransmitters are upregulated in human NAFLD and modulate the fibrogenic function of hepatic stellate cells. PLoS One 2013; 8: e72928.

27. Thullbery MD, Cox HD, Schule T, Thompson CM, George KM. Differential localization of acetylcholinesterase in neuronal and non-neuronal cells. J Cell Biochem 2005; 96: 599-610.

28. Clement S, Peyrou M, Sanchez-Pareja A, Bourgoin L, Ramadori P, Suter D, et al. Down-regulation of phosphatase and tensin homolog by hepatitis C virus core 3a in hepatocytes triggers the formation of large lipid droplets. Hepatology 2011; 54: 38-49.

29. Bolasco G, Calogero R, Carrara M, Banchaabouchi MA, Bilbao D, Mazzoccoli G, et al. Cardioprotective mIGF-1/SIRT1 signaling induces hypertension, leukocytosis and fear response in mice. Aging (Albany NY) 2012; 4: 402-416.

30. Intraobserver and interobserver variations in liver biopsy interpretation in patients with chronic hepatitis C. The French METAVIR Cooperative Study Group. Hepatology 1994; 20: 15-20.

31. Barathi VA, Weon SR, Beuerman RW. Expression of muscarinic receptors in human and mouse sclera and their role in the regulation of scleral fibroblasts proliferation. Mol Vis 2009; 15: 1277-1293.

32. Racke K, Juergens UR, Matthiesen S. Control by cholinergic mechanisms. Eur J Pharmacol 2006; 533: 57-68.

33. Cassiman D, Libbrecht L, Sinelli N, Desmet V, Denef C, Roskams T. The vagal nerve stimulates activation of the hepatic progenitor cell compartment via muscarinic acetylcholine receptor type 3. Am J Pathol 2002; 161: 521-530.

34. Bernard V, Brana C, Liste I, Lockridge O, Bloch B. Dramatic depletion of cell surface m2 muscarinic receptor due to limited delivery from intracytoplasmic stores in neurons of acetylcholinesterase-deficient mice. Mol Cell Neurosci 2003; 23: 121-133.

35. Matthiesen S, Bahulayan A, Holz O, Racke K. MAPK pathway mediates muscarinic receptor-induced human lung fibroblast proliferation. Life Sci 2007; 80: 2259-2262.

36. Psyrri A, Arkadopoulos N, Vassilakopoulou M, Smyrniotis V, Dimitriadis G. Pathways and targets in hepatocellular carcinoma. Expert Rev Anticancer Ther 2012; 12: 1347-1357.

37. Vinciguerra M, Foti M. PTEN at the crossroad of metabolic diseases and cancer in the liver. Ann Hepatol 2008; 7: 192-199.

38. Zhou Q, Lui VW, Yeo W. Targeting the PI3K/Akt/mTOR pathway in hepatocellular carcinoma. Future Oncol 2011; 7: 1149-1167.

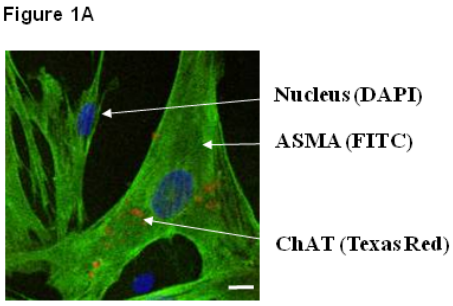

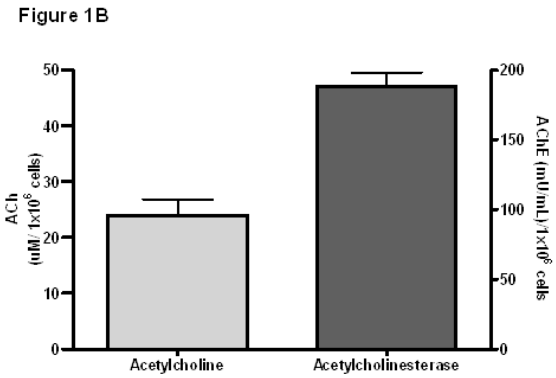

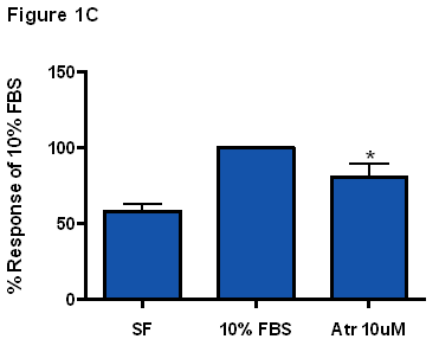

Fig. 1. Hepatic stellate cells express choline acetyltrasferase (ChAT), and secrete acetylcholine (ACh) and acetylcholinesterase (AChE), and require ACh as an endogenous growth factor**.** (A) Immunocytochemistry showing activated hHSC express ASMA (FITC) and ACh synthesising enzyme ChAT (Texas Red) (scale line 10μM). (B) Activated hHSC synthesise and release ACh and AChE. ACh is required for hHSC basal cell growth. (C) Atr 10uM inhibited hHSC basal growth 20% +/- 7% compare to FBS control. Experiments were performed in duplicate from 3 separate experiments. *: $p < 0.05$.

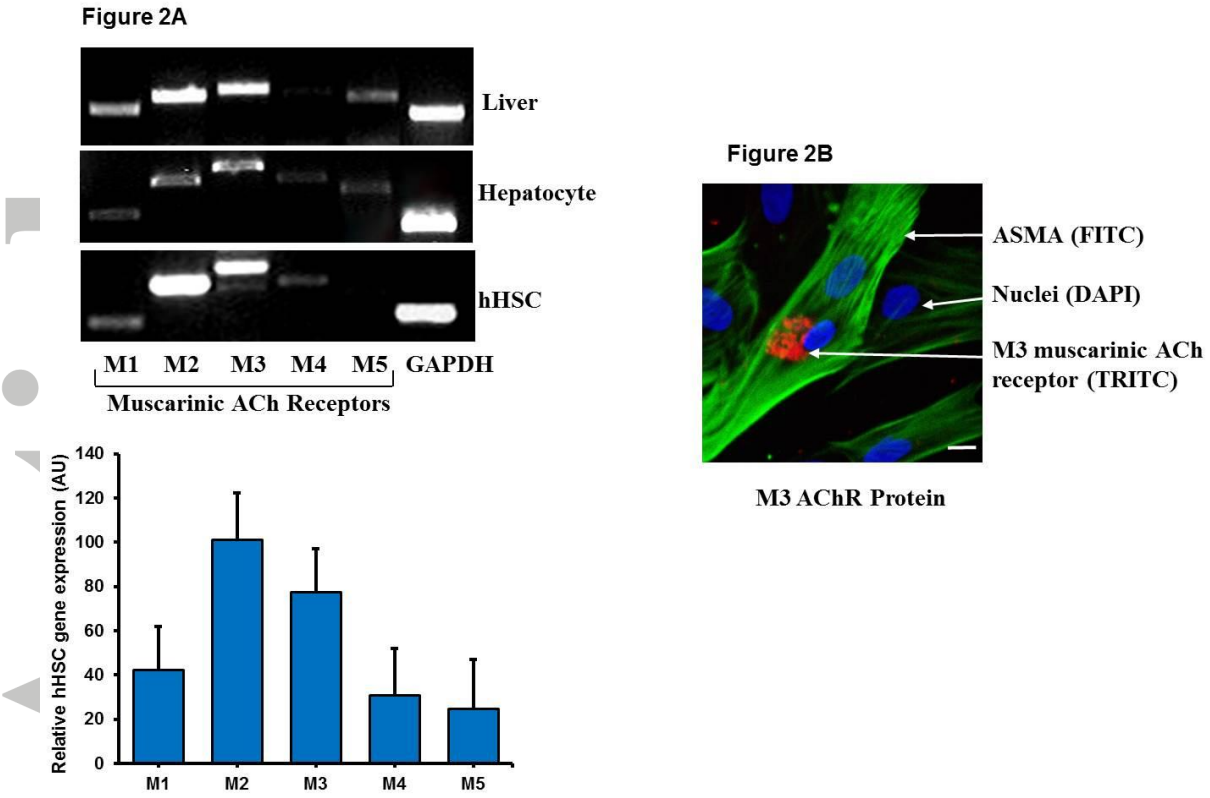

Fig. 2. hHSC, hepatocytes and whole liver express all mAChR. (A) Day 15 activated hHSC express M2 > M3 > M1 > M4 > M5 mRNA. While hepatocytes express mRNA for M3=M2 > M1=M4=M5 and whole liver with F4 fibrosis express mRNAs M2 > M3 > M1 > M5 > M4. Samples were amplified by real time-PCR and electrophoresis performed on 1.5% agarose gel, 90V, 60 mins. hHSC results were also expressed as bar graphs. (B) Confocal microscopy of activated HSC showed the cells express M3 mAChR protein (Texas Red fluorescence) with ASMA (FITC) proving activated HSC phenotype (scale line 10μM). Experiments were performed in duplicate from 3 separate experiments.

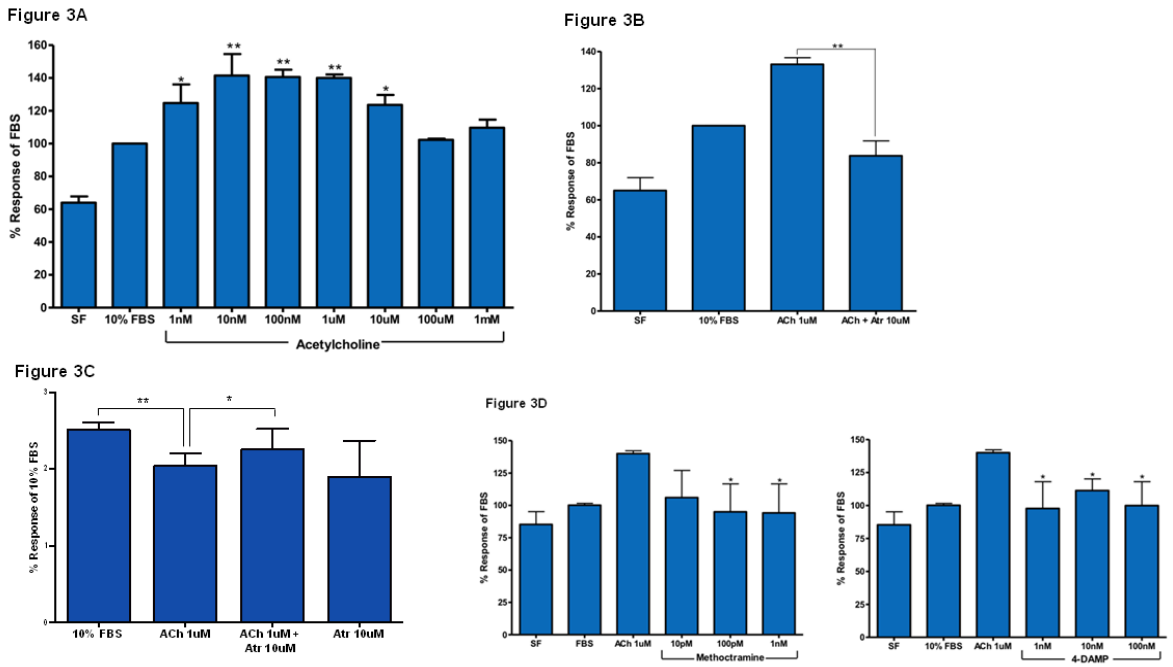

Fig. 3. Acetylcholine stimulates hHSC proliferation upstream via M2 and M3 ($G_{\alpha q/11}$ protein) mAChR, compared to FBS stimulated experimental group. (A) ACh 1uM induced hHSC proliferation in a dose dependent manner, with peak proliferation occurring at 10nM – 1uM increased to 140% +/- 2% of the FBS control. (B) ACh 1uM induced hHSC proliferation was blocked by Atr 10uM to 90.7% +/-8% of FBS control. (C) Human HSC exposed to ACh 1uM showed decreased stellate cell apoptosis by 21% +/- 2.8% when compared to FBS group. This effect was blocked when ACh 1uM and Atr 10uM were applied simultaneously. (D) Methoctramine inhibited ACh 1uM induced proliferation from 140 +/- 2% to 95 +/- 20% of FBS control while 4-DAMP inhibited ACh induced proliferation to 98 +/-18% of FBS control. Experiments were performed in duplicate from 3 separate experiments. *: $p < 0.05$; **: $p < 0.01$.

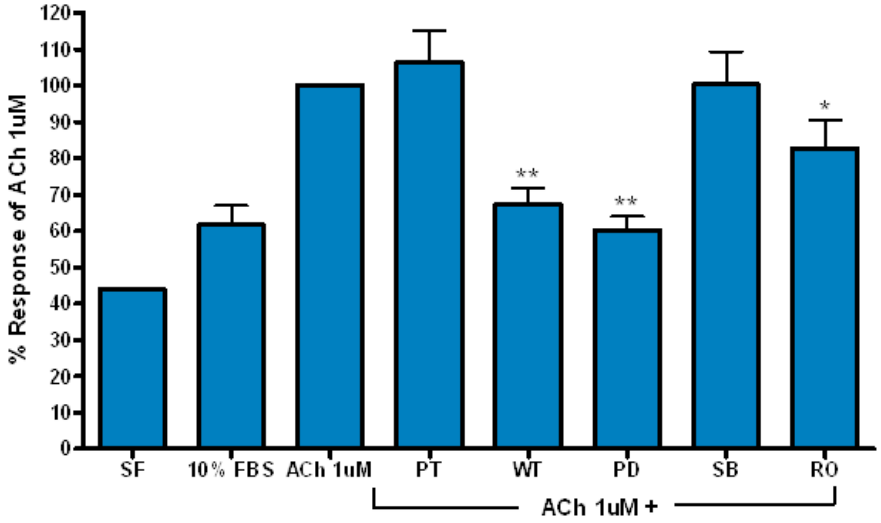

Fig. 4. hHSC exposed to ACh 1 µM as well as antagonist to $G_{\alpha i/o}$-protein, PI3-kinase, MEK, p38MAP-kinase, and PKC showed that both the PI3-K and MEK antagonists (WT and PD) inhibited Ach 1 µM induced proliferation by 35 +/- 5% and 42 +/- 4%. Proliferation was also inhibited by PKC antagonist (RO) 20 +/- 8%**).** Experiments were performed in duplicate from 3 separate experiments. *: $p < 0.05$; **: $p < 0.01$.

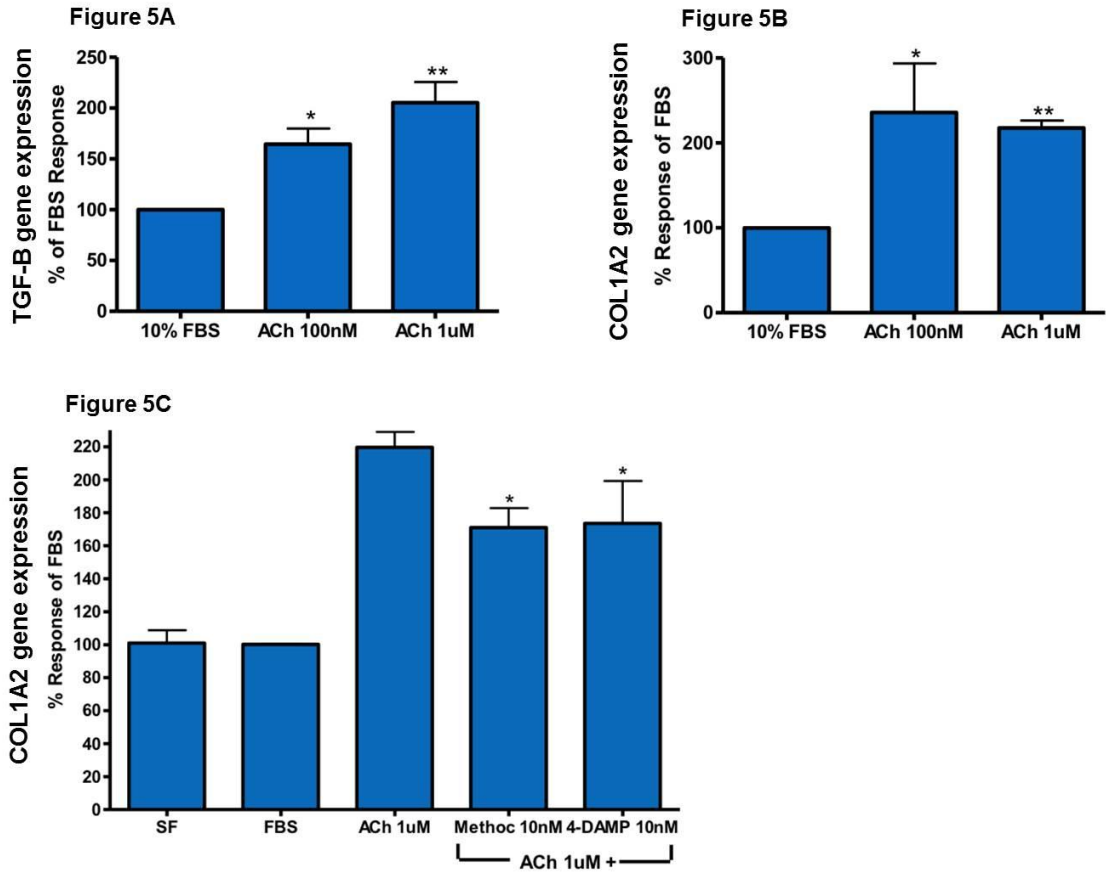

Fig. 5. ACh stimulation during 48 hours increased expression of fibrotic markers TGF-β and COL1A2 in hHSC, which is inhibited by 24 hours incubation together with M2 and M3 AChR antagonists. (A) hHSC exposed to ACh 100nM and 1uM had increased TGF-β gene expression up to 200% +/- 23.4% of the FBS control. (B) COL1A2 gene expression increased to 208% +/- 8.8% of the FBS control. (C) This effect was reduced by Methoctramine and 4-DAMP from 208% +/- 8.8% to 170 +/- 9% and 173 +/- 21% of the FBS control. Expression was determined by real time RT PCR and samples were standardised to GAPDH. Experiments were performed in duplicate from 3 separate experiments. (*: $p < 0.05$; **: $p < 0.01$).

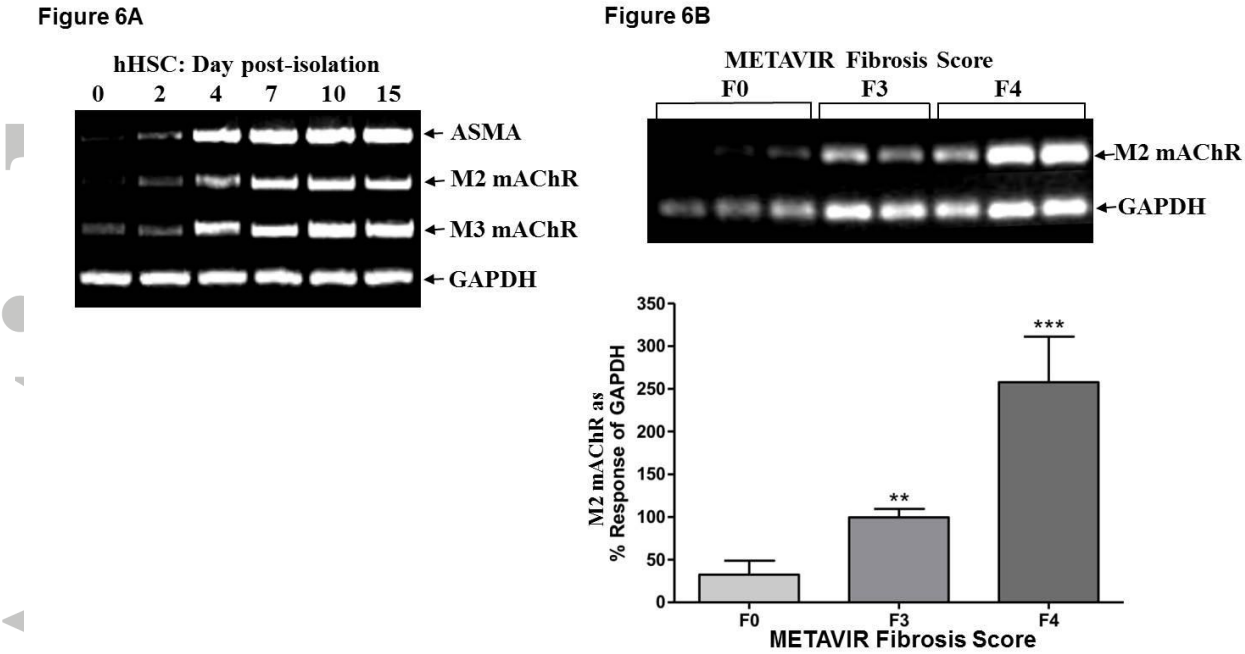

Fig. 6. M2 is upregulated in hHSC as well as in NASH fibrosis. (A) Isolated RNA from primary hHSC shows mRNAs for ASMA increased with cell activation time as did mRNAs for M2 and M3 AChR. (B) Whole liver biopsy samples from patients diagnosed with NASH and scored for fibrosis using the METAVIR fibrosis scoring system were analysed for ASMA, M2 and M3 mAChR. M2 expression increased from 38% +/- 12% in F0 samples to 250% +/- 48% in the F4 samples. Experiments were performed in duplicate from 3 separate experiments. **: $p < 0.01$; ***: $p < 0.001$.

Table 1. hHSC Drug Treatment

Drugs	Target and Action	Concentration
Acetylcholine (ACh)	muscarinic and nicotinic AChR agonist	1nM – 1mM
Atropine (Atr)	muscarinic AChR antagonist	10μM
Pertussis Toxin (PT)	inhibitor of $G_{\alpha i/o}$-proteins	100ng/mL
Wortmannin (WT)	inhibitor of PI3-K	100nM
PD 98059 (PD)	inhibitor of MEK	20μM
SB 202190 (SB)	inhibitor of p38 MAPK	10μM
RO 320432 (RO)	inhibitor of PKC	1μM
4-DAMP methiodide (4-DAMP)	M3 and M5 AChR antagonist	1nM – 100nM
Methoctramine hemihydrate (Methoc)	M2 AChR antagonist	10pM – 1nM

Table 2. Primer Sequences for QRT-PCR

Gene of Interest		Sequence (5' to 3')	Size (bp)	Annealing temp. (°C)
GAPDH	(for)	ACAGTCCATGCCATCACTGCC	320	55
	(rev)	GCCTGCTTCACCACCTTCTTG		
Muscarinic (M) AChR				
M1	(for)	CCGACTAAGAAAGGGCGTGA	313	57
	(rev)	GCAGCAGGCGAAAGGTGT		
M2	(for)	ACAAGAAGGAGCCTGTTGCCAACC	438	57
	(rev)	CAATCTTGCGGGCTACAATATTCTG		
M3	(for)	GACAGAAAACTTTGTCCACCCCAC	496	62
	(rev)	AGAAGTCTTAGCTGTGTCCACGGC		
M4	(for)	TCCTCAAGAGCCCACTAATGAAGC	430	59
	(rev)	TTCTTGCGCACCTGGTTGCGAGC		
M5	(for)	CTCACCACCTGTAGCAGCTACCC	397	59
	(rev)	CTCTCTTTCGTTTGGTCATTTGATG		
COL1A2	(for)	ATATTGCACCTTTGGACATC	236	55
	(rev)	TGCTCTGATCAATCCTTCTT		
TGF- β	(for)	AACCCACAACGAAATCTATG	157	55
	(rev)	GTGCTGCTCCACTTTTAACT		
ASMA	(for)	ACC CAC AAT GTC CCC ATC TA	300	55
	(rev)	TGA TCC ACA TCT GCT GGA AG		